Localization of Spin and Charge in Phenalenyl-Based Neutral Radical Conductors

ARTICLE *in* JOURNAL OF THE AMERICAN CHEMICAL SOCIETY · OCTOBER 2008

Impact Factor: 12.11 · DOI: 10.1021/ja8037307 · Source: PubMed

J|A|C|S
ARTICLES

Published on Web 09/18/2008

Localization of Spin and Charge in Phenalenyl-Based Neutral Radical Conductors

Robert C. Haddon,*,† Arindam Sarkar,† Sushanta K. Pal,† Xiaoliu Chi,‡ Mikhail E. Itkis,† and Fook S. Tham†

Departments of Chemistry and Chemical and Environmental Engineering, University of California, Riverside, California 92521-0403

Received May 19, 2008; E-mail: haddon@ucr.edu

Abstract: We report the development of an experimentally based structural analysis to examine the degree of localization of the spin and charge in the phenalenyl-based neutral radical molecular conductors—the results motivate a reinterpretation of the electronic structure of a number of the radicals that we have reported over the past 10 years. The analysis is based on the well-known relationship between bond order and bond length and makes use of the experimental bond distance deviations between the molecular structure of the radical and its corresponding cation. We determined the single crystal X-ray structure of the ethyl radical (**1**) at 11 temperatures between 90 K and room temperature so that we could follow the evolution of the structure and the electron density distribution through the magnetic phase transition that occurs in the vicinity of 140K. We show that the enhanced conductivity in the dimeric ethyl (**1**) and butyl (**3**) radicals at the magnetic phase transition results from the development of a complex, but highly delocalized electronic structure and not to the formation of a diamagnetic π-dimer. We find that the monomeric radicals **4**, **12**, and **13** have an asymmetric electron density distribution in the crystal lattice whereas radical **11** is the only monomeric radical which remains fully delocalized. The π-chain radicals (**7**, **8**, **14**, and **15**) retain the strongly delocalized electronic structures expected for a resonating valence bond ground-state structure.

Introduction

Originally organic compounds were viewed as insulators with low conductivity, but developments over the last 50 years have changed this perspective. Most of the current organic conductors and superconductors are based on charge-transfer salts that require electron transfer between two components (donor and acceptor) to generate charge carriers.[1−5] Molecular conductors based on neutral radicals represent an alternative approach to conventional charge-transfer organic conductors and superconductors in which the unpaired electron of the neutral radicals serves as the charge carrier.[6,7] Phenalenyl (PLY) is an odd alternant hydrocarbon with high symmetry (D_{3h}) that has the ability to form three redox species: cation, radical and anion.[8−10] The idea of using the phenalenyl system as the building block for designing an intrinsic molecular conductor and superconductor is challenging and this system has attracted theoretical and experimental attention,[11−25] although heterocyclic radicals have also been pursued.[26−31]

In our pursuit of phenalenyl-based neutral radical molecular conductors, we have used N- and O-functionalization to create three families of spiro-bis(1,9-disubstituted phenalenyl) boron radicals and one tris(1,9-disubstituted phenalenyl) silicon neutral radical (**1**−**15**, Scheme 1). The spiro-conjugation at the boron center leads to an intramolecular $\pi-\pi$ energy level splitting, and the lower level becomes a singly occupied molecular orbital (SOMO). Unlike conventional neutral radicals, in the solid state the spiro-conjugated biphenalenyls give rise to a quarter-filled energy band, and this significantly reduces the on-site Coulomb correlation energy (U), which is usually responsible for the insulating ground-state that occurs in half-filled band structures. The nonplanar geometry of these multicentered radicals inhibits the one-dimensional π-stacking that is characteristic of many charge-transfer salts.

We discovered the first phenalenyl-based neutral radical molecular conductor (**4**) in 1999, and we were surprised to find a crystal structure composed of monomeric radicals which exhibited no intermolecular contacts within van der Waals

† University of California.
‡ Present address: Department of Chemistry, Texas A&M University, Kingsville, TX 78363.

(1) Kepler, R. G.; Bierstedt, P. E.; Merrifield, R. E. *Phys. Rev. Lett.* **1960**, *5*, 503–504.
(2) Bechgaard, K.; Cowan, D. O.; Bloch, A. N. *J. Chem. Soc. Chem. Commun.* **1974**, 937–938.
(3) Parkin, S. S. P.; Engler, E. M.; Schumaker, R. R.; Lagier, R.; Lee, V. Y.; Scott, J. C.; Greene, R. L. *Phys. Rev. Lett.* **1983**, *50*, 270–273.
(4) Haddon, R. C.; et al. *Nature* **1991**, *350*, 320–322.
(5) Hebard, A. F.; Rosseinsky, M. J.; Haddon, R. C.; Murphy, D. W.; Glarum, S. H.; Palstra, T. T. M.; Ramirez, A. P.; Kortan, A. R. *Nature* **1991**, *350*, 600–601.
(6) Haddon, R. C. *Nature* **1975**, *256*, 394–396.
(7) Haddon, R. C. *Aust. J. Chem.* **1975**, *28*, 2343–2351.
(8) Reid, D. H. *Quart. Rev.* **1965**, *19*, 274–302.
(9) Reid, D. H. *Chem. Ind.* **1956**, 1504–1505.
(10) Reid, D. H. *Tetrahedron* **1958**, *3*, 339–352.
(11) Goto, K.; Kubo, T.; Yamamoto, K.; Nakasuji, K.; Sato, K.; Shiomi, D.; Takui, T.; Kubota, M.; Kobayashi, T.; Yakusi, K.; Ouyang, J. *J. Am. Chem. Soc.* **1999**, *121*, 1619–1620.
(12) Fukui, K.; Sato, K.; Shiomi, D.; Takui, T.; Itoh, K.; Gotoh, K.; Kubo, T.; Yamamoto, K.; Nakasuji, K.; Naito, A. *Synth. Met.* **1999**, *103*, 2257–2258.
(13) Koutentis, P. A.; Chen, Y.; Cao, Y.; Best, T. P.; Itkis, M. E.; Beer, L.; Oakley, R. T.; Brock, C. P.; Haddon, R. C. *J. Am. Chem. Soc.* **2001**, *123*, 3864–3871.

Scheme 1

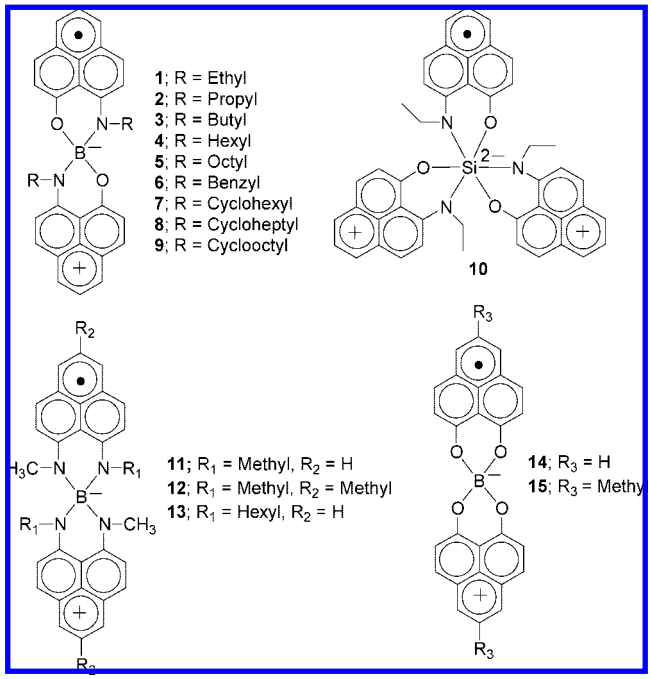

atomic separation.[32] Magnetic susceptibility measurements of **4** supported the picture of isolated molecules in the crystal lattice by showing Curie behavior (1 spin per molecule), throughout the temperature range 10−400 K, thereby confirming the presence of noninteracting spins in the solid state. Nevertheless the compound showed a room-temperature conductivity of $\sigma_{RT} = 0.05$ S/cm, the highest yet for a neutral radical conductor and we suggested that the ground-state of the radical was best represented as a degenerate Mott-Hubbard insulator. Since that time we have only found three other radicals that approached the monomeric structure of **4**, and these compounds derive from the (N, N) ligand system.[33] The compounds have very weak intermolecular interactions in the solid state, and the magnetic susceptibility could be fit to the Curie−Weiss function with $\theta = -55$ (**11**), -70 (**12**,) and -14K (**13**), or to the antiferromagnetic 1-D Heisenberg model; the intermolecular contacts are at or beyond the van der Waals separation and the conductivities span a broad range: $\sigma_{RT} = 0.04$ (**11**), 0.01 (**12**), and 7×10^{-6} S/cm (**13**).

Shortly after the synthesis of the n-hexyl-substituted radical **4** we investigated shorter chain analogs, and found that the ethyl (**1**) and butyl (**3**) compounds crystallize as face-to-face π-dimers so that there is selective registry between spin-bearing carbon atoms of the phenalenyl units; the separation between dimers is still well outside of the van der Waals distances supporting the idea of a localized electronic structure, although the compounds showed conductivities of $\sigma_{RT} = 0.01$ (**1**), and 0.02 (**3**) S/cm.[34] These dimeric neutral radicals (**1** and **3**) simultaneously exhibit bistability in three physical channels: magnetic, electrical and optical, which has been rarely realized in a single system.[35,36] The crystals undergo phase transitions from high temperature paramagnetic states to low temperature diamagnetic states, accompanied by an increase in the conductivities by 2 orders of magnitude. The propyl radical (**2**) crystallizes as a weakly bound, paramagnetic π-dimer but the conductivity of this compound ($\sigma_{RT} = 1 \times 10^{-6}$ S/cm), is much lower than that of **1** and **3** because of the orientation of the molecules in the crystal lattice.[37] The n-octyl (**5**) and cyclooctyl (**9**) radicals can be crystallized as both a σ-dimer and a π-dimer—these latter structures are weakly bound (paramagnetic, **5**) and strongly bound (diamagnetic, **9**) dimers; both compounds show low conductivity: $\sigma_{RT} = 1 \times 10^{-5}$ (**5**), and 1×10^{-6} S/cm (**9**).[38,39] Recently we crystallized the first tris-phenalenyl-based neutral radical (**10**), which proved to be a weak π-dimer in which the unpaired electrons populate nondimerized phenalenyl units and thus gives rise to a paramagnetic structure of low conductivity: $\sigma_{RT} = 2 \times 10^{-6}$ S/cm (**10**).[40]

Apart from the structural motifs discussed above we have found a number of 1D- and pseudo-1D-neutral radical conductors; the first of these was the benzyl compound (**6**) which crystallized in an unusual π-step structure involving lateral overlap of just 4 of the 12 active carbon atoms with large coefficients in the SOMO. The magnetism of this compound

(14) Morita, Y.; Aoki, T.; Fukui, K.; Nakazawa, S.; Tamaki, K.; Suzuki, S.; Fuyuhiro, A.; Yamamoto, K.; Sato, K.; Shiomi, D.; Naito, A.; Takui, T.; Nakasuji, K. *Angew. Chem., Int. Ed.* **2002**, *41*, 1793–1796.
(15) Takano, Y.; Taniguchi, T.; Isobe, H.; Kubo, T.; Morita, Y.; Yamamoto, K.; Nakasuji, K.; Takui, T.; Yamaguchi, K. *J. Am. Chem. Soc.* **2002**, *124*, 11122–11130.
(16) Takano, Y.; Taniguchi, T.; Isobe, H.; Kubo, T.; Morita, Y.; Yamamoto, K.; Nakasuji, K.; Takui, T.; Yamaguchi, K. *Chem. Phys. Lett.* **2002**, *358*, 17–23.
(17) Zheng, S.; Lan, J.; Khan, S. I.; Rubin, Y. *J. Am. Chem. Soc.* **2003**, *125*, 5786–5791.
(18) Huang, J.; Kertesz, M. *J. Am. Chem. Soc.* **2003**, *125*, 13334–13335.
(19) Small, D.; Zaitsev, V.; Jung, Y.; Rosokha, S. V.; Head-Gordon, M.; Kochi, J. K. *J. Am. Chem. Soc.* **2004**, *126*, 13850–13858.
(20) Zheng, S.; Thompson, J. D.; Tontcheva, A.; Khan, S. I.; Rubin, Y. *Org. Lett.* **2005**, *7*, 1861–1863.
(21) Zaitsev, V.; Rosokha, S. V.; Head-Gordon, M.; Kochi, J. K. *J. Org. Chem.* **2006**, *71*, 520–526.
(22) Huang, J.; Kertesz, M. *J. Am. Chem. Soc.* **2006**, *128*, 1418–1419.
(23) Huang, J.; Kertesz, M. *J. Am. Chem. Soc.* **2006**, *128*, 7277–7286.
(24) Huang, J.; Kertesz, M. *J. Am. Chem. Soc.* **2007**, *129*, 1634–1643.
(25) Huang, J.; Kertesz, M. *J. Phys. Chem. A* **2007**, *111*, 6304–6315.
(26) Oakley, R. T. *Can. J. Chem.* **1993**, *71*, 1775–1784.
(27) Andrews, M. P.; Cordes, A. W.; Douglass, D. C.; Fleming, R. M.; Glarum, S. H.; Haddon, R. C.; Marsh, P.; Oakley, R. T.; Palstra, T. T. M.; Schneemeyer, L. F.; Trucks, G. W.; Tycko, R.; Waszczak, J. V.; Young, K. M.; Zimmerman, N. M. *J. Am. Chem. Soc.* **1991**, *113*, 3559.
(28) Cordes, A. W.; Haddon, R. C.; Oakley, R. T.; Schneemeyer, L. F.; Waszczak, J. V.; Young, K. M.; Zimmerman, N. M. *J. Am. Chem. Soc.* **1991**, *113*, 582–588.
(29) Leitch, A. A.; Reed, R. W.; Robertson, C. M.; Britten, J. F.; Yu, X.; Secco, R. A.; Oakley, R. T. *J. Am. Chem. Soc.* **2007**, *129*, 7903–7914.
(30) Robertson, C. M.; Leitch, A. A.; Cvrkalj, K.; Reed, R. W.; Myles, D. J. T.; Dube, P. A.; Oakley, R. T. *J. Am. Chem. Soc.* **2008**, *130*, 8414–8425.
(31) Hicks, R. G. *Org. Biomol. Chem.* **2007**, *5*, 1321–1338.
(32) Chi, X.; Itkis, M. E.; Patrick, B. O.; Barclay, T. M.; Reed, R. W.; Oakley, R. T.; Cordes, A. W.; Haddon, R. C. *J. Am. Chem. Soc.* **1999**, *121*, 10395–10402.
(33) Mandal, S. K.; Itkis, M. E.; Chi, X.; Samanta, S.; Lidsky, D.; Reed, R. W.; Oakley, R. T.; Tham, F. S.; Haddon, R. C. *J. Am. Chem. Soc.* **2005**, *127*, 8185–8196.
(34) Chi, X.; Itkis, M. E.; Kirschbaum, K.; Pinkerton, A. A.; Oakley, R. T.; Cordes, A. W.; Haddon, R. C. *J. Am. Chem. Soc.* **2001**, *123*, 4041–4048.
(35) Itkis, M. E.; Chi, X.; Cordes, A. W.; Haddon, R. C. *Science* **2002**, *296*, 1443–1445.
(36) Miller, J. S. *Angew. Chem., Int. Ed* **2003**, *42*, 27–29.
(37) Chi, X.; Itkis, M. E.; Reed, R. W.; Oakley, R. T.; Cordes, A. W.; Haddon, R. C. *J. Phys. Chem. B* **2002**, *106*, 8278–8287.
(38) Liao, P.; Itkis, M. E.; Oakley, R. T.; Tham, F. S.; Haddon, R. C. *J. Am. Chem. Soc.* **2004**, *126*, 14297–14302.
(39) Pal, S. K.; Itkis, M. E.; Tham, F. S.; Reed, R. W.; Oakley, R. T.; Donnadieu, B.; Haddon, R. C. *J. Am. Chem. Soc.* **2007**, *129*, 7163–7174.
(40) Pal, S. K.; Itkis, M. E.; Tham, F. S.; Reed, R. W.; Oakley, R. T.; Haddon, R. *J. Am. Chem. Soc.* **2008**, *130*, 3942–3951.

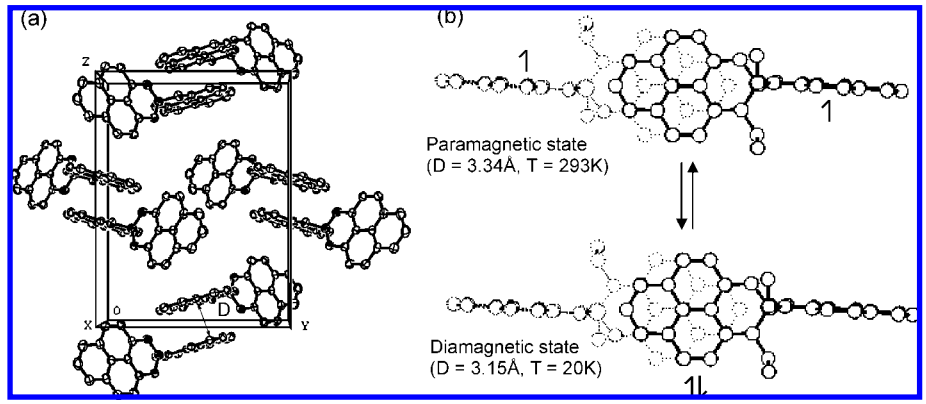

Figure 1. (a) Unit cell of the ethyl radical (**1**) showing pairs of π-dimers,[34] with ethyl groups omitted, where D is the mean plane separation. (b) Overlap between the two molecules of a π-dimer showing the previously determined location of the unpaired electrons.[35,46]

could be fit to a one-dimensional $S = {}^1/_2$ antiferromagnetic Heisenberg chain model with $J = -52.3$ cm^{-1}. However, given the absence of a structural instability, such as a charge density wave state, the nonmetallic character of the conductivity [$\sigma_{RT} = 1 \times 10^{-3}$ S/cm (**6**)] was difficult to explain and we were unable to provide a self-consistent account of the electronic structure of the compound.[41] We subsequently realized that the resonance structures provided in this paper are best interpreted in terms of a resonating valence bond (RVB) ground state[39,42−44] for this compound and this description is also applicable to the π-chain structures found for compounds **7**, **8**, **14**, and **15** which essentially crystallize as infinitely repeating forms of the π-dimers **1** and **3**. These compounds were also stable in their highly symmetric 1-D structures and gave rise to some of the highest conductivities attained for this class of compounds: $\sigma_{RT} = 0.3$ (**7**), 0.1 (**14**), and 0.3 S/cm (**15**).[39,44,45]

Thus it is apparent that the multifunctional phenalenyl neutral radical conductors offer a variety of electronic and solid state structures in which the (de)localization of the spin and charge is of paramount importance. The ethyl and butyl radicals (**1** and **3**) form π-dimers, with the active carbon atoms superimposed (Figure 1) in order to maximize the overlap between the singly occupied molecular orbitals (SOMOs). However, the magnetic susceptibility measurements indicate that these radicals are diamagnetic only at low temperatures; as the temperature is raised they undergo a phase transition to paramagnetic dimers, suggesting that the two unpaired electrons which are involved in the π-dimer, must dissociate at high temperatures.[34,35] To understand these results, we developed a method that allows us to qualitatively ascertain the location of the unpaired electrons.[46] This method was based on the characteristics of the SOMO (Figure 2); in particular the signs of the partial bond orders (product of the coefficients between neighboring atoms in the SOMO). A positive partial bond order indicates the bond should be strengthened if the SOMO is occupied by an unpaired electron in the SOMO of the radical and thus should be shorter

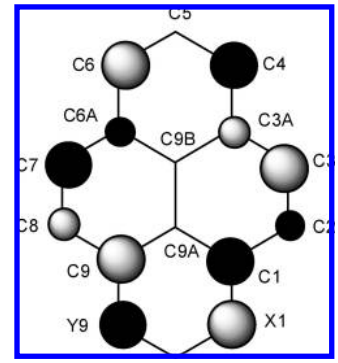

Figure 2. SOMO of half of the 1,9-disubstituted-phenalenyl boron radical (LUMO in the case of the cation).[47]

than that of the corresponding cation (without the unpaired electron). Conversely, a negative partial bond order will led to a weaker bond and a longer bond length, if the SOMO is populated by an unpaired electron. Thus a comparison of the bond lengths of a particular PLY unit (in cation and radical) together with knowledge of the signs of the partial bond orders, allows an assignment of the location of the unpaired electron. By using this method, we discovered that in the low temperature regime, the unpaired electrons in **1** and **3** reside in the superimposed PLY rings (Figure 1b, lower part), and undergo spin pairing to form a π-dimer; whereas above the magnetic phase transition temperature the unpaired electrons avoid each other and localize in the nonsuperimposed PLY units (Figure 1b, top part). This information allowed a rationalization of the structural transition and the magnetic properties but the increase in conductivity below the phase transition has remained unexplained.

Thus, in the case of **1** and **3** it has been assumed that the unpaired electron on each molecule is always localized in a single PLY unit.[35,46] On the other hand, solution phase electrochemical and ESR measurements show that the two PLY units of **14** are electronically connected through spiro-conjugation so that the unpaired electron effectively delocalizes over the whole molecule[47] and this delocalized electronic structure is characteristic of solid state **4**, **6**, **7**, **8**, **11**−**15**. Furthermore, our recent synthetic progress has led to a range of compounds with complicated structures, such as tris-phenalenyl silicon radicals (**10**),[40] and it is desirable to have a quantitative method

(41) Pal, S. K.; Itkis, M. E.; Reed, R. W.; Oakley, R. T.; Cordes, A. W.; Tham, F. S.; Siegrist, T.; Haddon, R. C. *J. Am. Chem. Soc.* **2004**, *126*, 1478–1484.
(42) Pauling, L. *Nature* **1948**, *161*, 1019–1020.
(43) Anderson, P. W. *Mater. Res. Bull.* **1973**, *8*, 153–160.
(44) Pal, S. K.; Itkis, M. E.; Tham, F. S.; Reed, R. W.; Oakley, R. T.; Haddon, R. C. *Science* **2005**, *309*, 281–284.
(45) Mandal, S. K.; Samanta, S.; Itkis, M. E.; Jensen, D. W.; Reed, R. W.; Oakley, R. T.; Tham, F. S.; Donnadieu, B.; Haddon, R. C. *J. Am. Chem. Soc.* **2006**, *128*, 1982–1994.
(46) Chi, X.; Tham, F. S.; Cordes, A. W.; Itkis, M. E.; Haddon, R. C. *Synth. Met.* **2003**, *133*−*134*, 367–372.
(47) Haddon, R. C.; Chichester, S. V.; Marshall, J. H. *Tetrahedron* **1986**, *42*, 6293–6300.

Scheme 2. Illustration of the Limiting Cases for **14**[a]

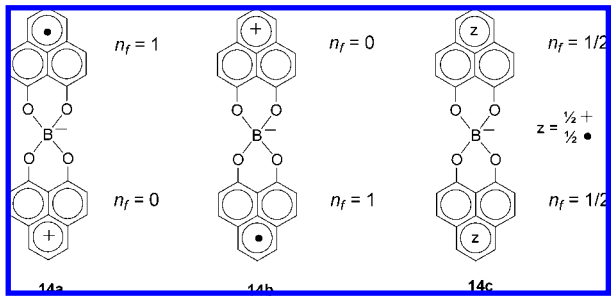

[a] Orbital occupancies (n_f) for the two frontier molecular orbitals (FMOs), in the two possible localized electronic structures (**14a** and **14b**), and the fully delocalized electronic structure (**14c**).

of assigning the electron distribution among the PLY units within a molecule; thus it is the purpose of the present manuscript to develop such an analysis and to re-examine the degree of (de)localization of the spin and charge in these solid state radicals.

Methodology. As noted above, we previously utilized experimental bond length data to provide information on the location of the odd electron in the 1,9-disubstituted-phenalenyl boron radicals,[46] by a qualitative analysis of the bond orders of the lowest unoccupied molecular orbital (LUMO) of the cations [equivalent to the singly occupied molecular orbital (SOMO) of the radicals]. In this section we extend this approach in order to devise a quantitative analysis of the electron density distribution in these radicals by making use of the well-known linear dependence between bond length [r_{kl}(Å)] and bond order [p_{kl}] among pairs of atoms k and l within the Hückel Molecular Orbital (HMO) theory of conjugated π-electron systems.[48−50] The bond order depends on the molecular orbital coefficients:

$$p_{kl} = \sum_j n_j p_{kl}^{(j)} = \sum_j n_j c_{jk} c_{jl} \tag{1}$$

Where $p_{kl}^{(j)} (= c_{jk}c_{jl})$ is the partial bond order between atoms k and l, and n_j is the occupancy (taken to lie in the range 0−2), of molecular orbital j. In the present case, we are interested in the occupancy of what has been referred to as the radical SOMO, that is, the molecular orbital that may be occupied by the unpaired electron, but in these multicentered phenalenyl radicals the SOMO can be highly delocalized or it can be localized on any one of at least two phenalenyl systems. Thus we shall refer to the (potential) SOMOs as the frontier molecular orbitals (FMO, f), and our interest will be in using the partial bond orders $p_{kl}^{(f)}$ to determine the orbital occupancies n_f of the FMOs and thus the (de)localization of the electron spin in the radicals, as exemplified in Scheme 2 for **14**.

Traditionally the linear relationship between bond order and bond length is expressed as

$$r_{kl} = Ap_{kl} + B \tag{2}$$

Depending on the compounds that are included in the analysis, various values for A and B have been reported in the literature—if the HMO bond orders of ethylene, benzene, and graphite are used to fit their experimental bond lengths then this equation gives values of $A = -0.18$ and $B = 1.517$ (Å).[49]

In the present connection we focus on the change in bond length (Δr_{kl}) that occurs as a result of the change in bond order (Δp_{kl}) if the FMO is populated, and thus eq 2 may be written

$$\Delta r_{kl} = A\Delta p_{kl} \tag{3}$$

Furthermore, in our analysis the real point of interest is the location(s) of the electron spin and thus we must solve for the occupancy of the individual FMOs (n_f, where $1 \geq n_f \geq 0$ and $\sum n_f = 1$, see Scheme 2), and thus we can write eq 3 in the form

$$\Delta r_{kl} = An_f p_{kl}^f \tag{4}$$

Thus a plot of Δr_{kl} against p_{kl}^f should yield a straight line which passes through the origin with a slope given by An_f for any FMO which is occupied and because $\sum n_f = 1$, the sum of the slopes of the individual FMOs in any given radical will give an independent estimate of A. In the present analysis, the partial bond orders (p_{kl}^f, × values) for the 3 types of disubstituted radicals [(N,O), (N,N), and (O,O)] were obtained from simple HMO calculations and the Δr_{kl} values (y) were obtained as the difference between the corresponding bond lengths in the radical

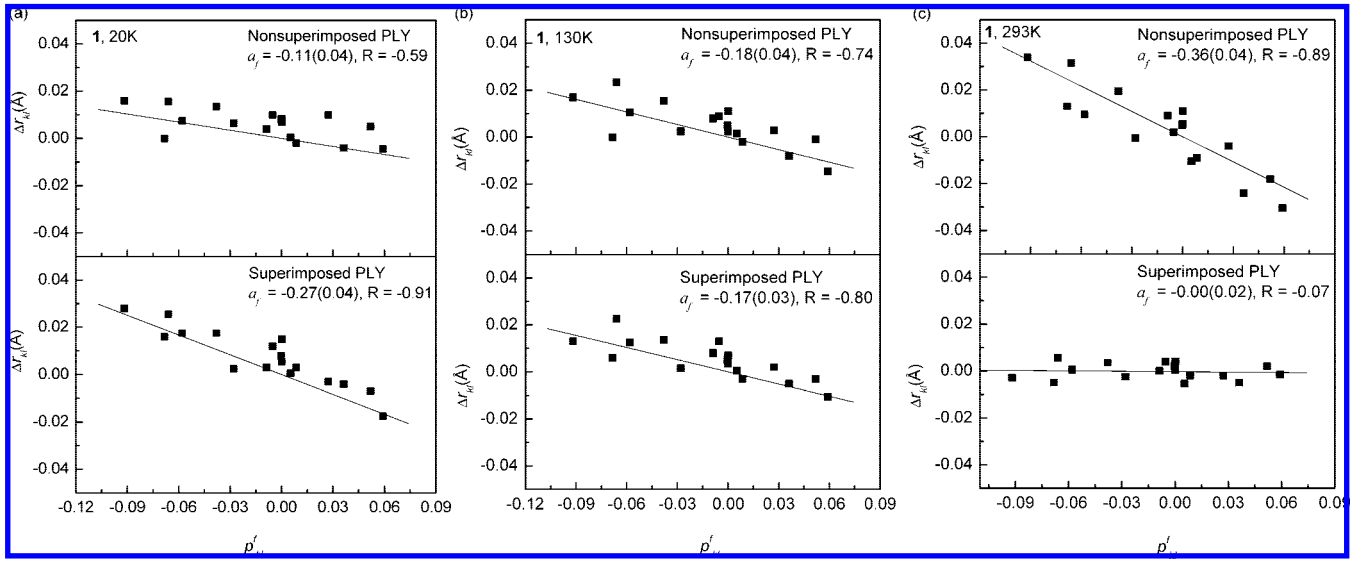

Figure 3. Plot of the change in bond order (p_{kl}^f) versus change in bond length (Δr_{kl}) for ethyl radical (**1**): (a) 20 K, electron is partially localized in the superimposed PLY units, (b) 130 K, electron is delocalized over the two PLY units, (c) 293 K, electron is in the nonsuperimposed PLY units (see Experimental Section and Supporting Information for Δr_{kl} values).

Table 1. Regression Analysis of Change in Bond Order against Change in Bond Length of Phenalenyl Units in Radical **1** (O, N-ethyl), Using Zero Intercept Fit of the form $y = a_f x$

T (K)	PLY environment	R^a	slope [a_i] (SD)[b]	sum of slopes	electron distribution[c]	D^d (Å)
20[e]	Superimposed	−0.91	−0.27 (0.04)	−0.38	0.71	3.15
	Nonsuperimposed	−0.59	−0.11 (0.04)		0.29	
90[f]	Superimposed	−0.85	−0.22(0.04)	−0.34	0.65	3.17
	Nonsuperimposed	−0.54	−0.12(0.04)		0.35	
100[f]	Superimposed	−0.87	−0.22(0.03)	−0.35	0.63	3.18
	Nonsuperimposed	−0.62	−0.13(0.04)		0.37	
110[f]	Superimposed	−0.86	−0.22(0.03)	−0.36	0.61	3.19
	Nonsuperimposed	−0.66	−0.14(0.04)		0.39	
120[f]	Superimposed	−0.85	−0.20(0.03)	−0.35	0.57	3.19
	Nonsuperimposed	−0.68	−0.15(0.04)		0.43	
130[f]	Superimposed	−0.80	−0.17(0.03)	−0.35	0.49	3.21
	Nonsuperimposed	−0.74	−0.18(0.04)		0.51	
135[f]	Superimposed	−0.77	−0.15(0.03)	−0.36	0.42	3.22
	Nonsuperimposed	−0.78	−0.21(0.04)		0.58	
140[f]	Superimposed	−0.38	−0.06(0.03)	−0.35	0.17	3.28
	Nonsuperimposed	−0.86	−0.29(0.04)		0.83	
150[f]	Superimposed	−0.30	−0.05(0.03)	−0.36	0.14	3.29
	Nonsuperimposed	−0.87	−0.31(0.04)		0.86	
160[f]	Superimposed	−0.24	−0.04(0.03)	−0.35	0.11	3.29
	Nonsuperimposed	−0.87	−0.31(0.04)		0.89	
170[f]	Superimposed	−0.11	−0.02(0.03)	−0.34	0.06	3.30
	Nonsuperimposed	−0.87	−0.32(0.04)		0.94	
293[f]	Superimposed	−0.07	−0.00(0.02)	−0.36	0	3.34
	Nonsuperimposed	−0.89	−0.36(0.04)		1	

[a] R = correlation coefficient. [b] Slope (a_f) obtained from the plot of Δr_{kl} against p^f_{kl}. [c] Electron distribution among the FMOs; determined by the ratio of the slope to the sum of the slopes, $a_f/\sum a_f$ (equivalent to $n_f/\sum n_f$). [d] D = Mean plane separation of the superimposed, or π-dimer PLY units. [e] X-ray structure from previous work.[34] [f] X-ray structure from this work.

and cation [exemplified in Scheme 2 for **14**, where $\Delta r_{kl}(\mathbf{14}) = r_{kl}(\mathbf{14}) - r_{kl}(\mathbf{14}^+)$, Calculation Section], and fit to the equation $y = a_f x$; the sum $\sum a_f$ provides an independent estimate of A.

Results and Discussion

To test the analysis we examined the structures of the ethyl radical (**1**), which we have previously characterized in the solid state.[34] We determined the single crystal X-ray structure of this compound at 11 additional temperatures between 90K and room temperature so that we could follow the evolution of the structure and the electron density distribution through the phase transition that occurs in the vicinity of 140K. Three representative plots of the change in bond length (Δr_{kl}, y) as a function of the change in bond order (p^f_{kl}, x) are shown in Figure 3 and the results of the regression analyses ($y = a_f x$), at all temperatures are listed in Table 1; the complete set of data is given in the Supporting Information. In those phenalenyl FMOs where there is appreciable electron density it is apparent that equation 4 provides a good description of the relationship between bond order and bond length as evidenced by the plots (Figure 3) and the correlation coefficients (R) given in Table 1. It is also apparent that the sum of the slopes ($\sum a_f$), provides a uniform estimate of the value of A [= −0.35 (0.01)], although the dependence of bond length on bond order is approximately twice that discussed above. Thus we examined the bond length−bond order relationship in a condensed aromatic hydrocarbon (ovalene), which is frequently cited as a model case for this type of correlation,[48,50] and obtained $A = -0.33$ (0.04), ($A = -0.27$ (0.02) using recent data, see Supporting Information) which supports the larger values shown in Table 1 and the mean value given above; thus we conclude that the structural analysis presented above can be used to provide quantitative information

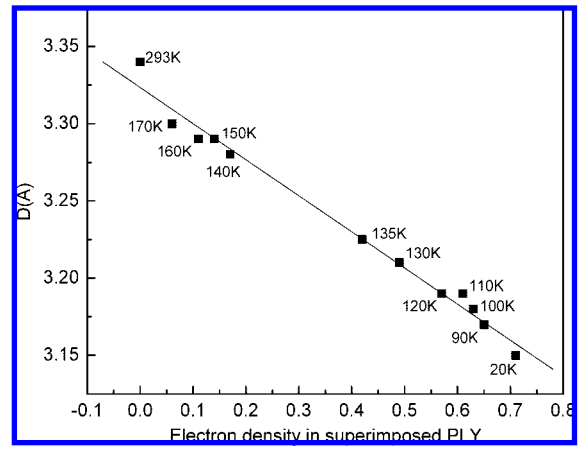

Figure 4. Graph of charge density in the superimposed PLY unit versus mean plane separation (D) in radical **1**.

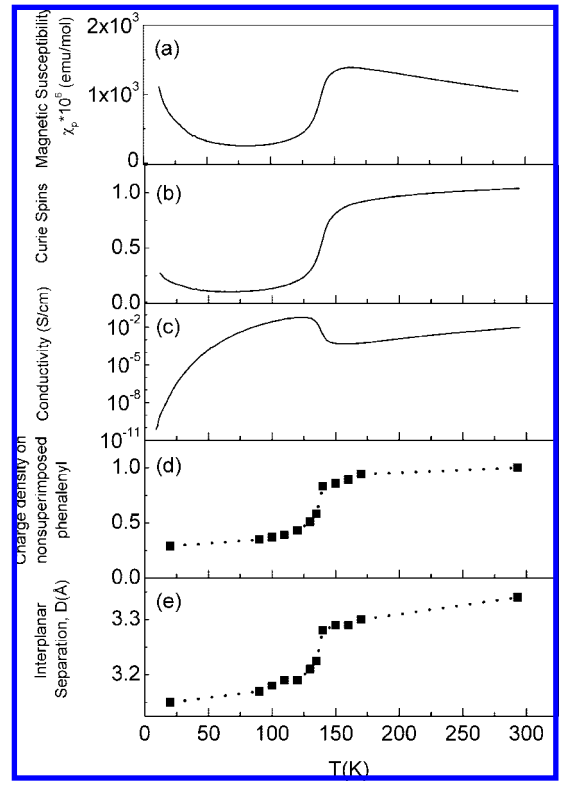

Figure 5. Physical measurements and analysis of (O, N-ethyl) radical (**1**) crystals as a function of temperature: (a) Paramagnetic susceptibility (χ_p), (b) fraction of Curie spins ($n = 8 \times \chi_p \times T/3$, calculated from the measured paramagnetism), (c) single-crystal conductivity, (d) calculated electron density in nonsuperimposed PLY and, (e) mean interplanar separation between superimposed PLY rings.

on the electron density distribution in the phenalenyl radicals (**1**−**15**), and in what follows we discuss the results of our investigation into the spin and charge density distributions of these compounds.

In our previous analysis of the ethyl radical (**1**), we rationalized the observed properties in terms of a high temperature structure (lower conductivity, paramagnetic and optically transparent) and a low temperature structure (high conductivity, diamagnetic and optically opaque). We associated the high temperature phase with a paramagnetic electronic structure in which the unpaired electron is localized in the nonsuperimposed phenalenyl rings and the low temperature structure with an

Table 2. Regression Analysis of Change in Bond Order against Change in Bond Length of Phenalenyl Units in Radicals **1**−**15**, Using Zero Intercept Fit of the form $y = a_f x$

radical	R^a	slope [a_f] (SD)	sum of slopes	structure[b]	T^c	PLY env[d]	D (Å)[e]	elect count[f]	elect dist[g]	$\sigma_{RT}{}^h$ (S/cm)
1	−0.91	−0.27(0.04)	−0.38	π-Dimer	20	S	3.15	1	0.71	1×10^{-2}
	−0.59	−0.11(0.04)				NS		0	0.29	
1	−0.07	−0.00(0.02)	−0.36	π-Dimer	293	S	3.34	0	0	1×10^{-2}
	−0.89	−0.36(0.04)				NS		1	1	
2	−0.10	0.00(0.03)	−0.40	π-Dimer	293	S	3.40	0	0	1×10^{-6}
	−0.90	−0.40(0.04)				NS		1	1	
3	−0.91	−0.33(0.04)	−0.33	π-Dimer	173	S	3.12	1	1	2×10^{-2}
	0.13	−0.00(0.02)				NS		0	0	
4	−0.78	−0.16(0.03)	−0.41	Monomer	173	PLY 1	(3.49)	0.5	0.39	5×10^{-2}
	−0.90	−0.25(0.03)				PLY 2		0.5	0.61	
5	0.24	0.08(0.06)[g]	−0.44	π-Dimer	223	S	3.40	0	0	1×10^{-5}
	−0.91	−0.44(0.07)				NS		1	1	
6	−0.67	−0.12(0.03)	−0.24	π-Step	223	PLY 1,2		0.5	0.50	1×10^{-3}
7	−0.94	−0.19(0.02)	−0.38	π-Chain	297	S	3.32	0.5	0.50	3×10^{-1}
8	−0.72	−0.19(0.04)	−0.38	π-Chain	100	S	3.26	0.5	0.50	2×10^{-3}
9	−0.94	−0.29(0.03)	−0.34	π-Dimer	100	S	3.16	1	0.85	1×10^{-6}
	−0.41	−0.05(0.02)				NS		0	0.15	
10	0.35	0.09(0.05)[g]	−0.44	π-Dimer	100	PLY 1	3.39	0	0	2×10^{-6}
	0.36	0.07(0.04)[g]				PLY 2		0	0	
	−0.88	−0.44(0.06)				PLY 3		1	1	
11	−0.87	−0.18(0.02)	−0.37	Monomer	218	PLY 1	(3.38)	0.5	0.49	4×10^{-2}
	−0.89	−0.19(0.02)				PLY 2		0.5	0.51	
12	−0.83	−0.29(0.05)	−0.48	Monomer	223	PLY 1	(3.43)	0.5	0.60	1×10^{-2}
	−0.81	−0.19(0.03)				PLY 2		0.5	0.40	
13	−0.91	−0.42(0.05)	−0.47	Monomer	223	PLY 1	(3.69)	0.5	0.89	7×10^{-6}
	−0.31	−0.05(0.03)				PLY 2		0.5	0.11	
14	−0.55	−0.20(0.08)	−0.40	π-Chain	100	S	3.17	0.5	0.50	1×10^{-1}
15	−0.66	−0.18(0.05)	−0.42	π-Chain	100	PS	3.29	0.5	0.43	3×10^{-1}
	−0.88	−0.24(0.03)				S	3.26	0.5	0.57	

[a] R = correlation coefficient. [b] Structure of the radical in the crystal lattice. [c] Temperature (K) of X-ray structure determination. [d] Phenalenyl environment: S = Superimposed, NS = Non superimposed, PS = Partially superimposed PLY. [e] D = Mean plane separation of the superimposed or π-dimer PLY units. In the case of monomeric radicals the closest distance between active carbon atoms is given in parentheses. [f] Formal electron assignment (based on previous work, see text). [g] Electron distribution among the FMOs of individual PLY units; determined by the ratio of the slope to sum of the slopes for all PLY units, $a_f/\sum a_f$ (equivalent to $n_f/\sum n_f$). Note that a positive slope does not have any physical significance in the bond order - bond length model. [h] σ_{RT} = Room temperature conductivity.

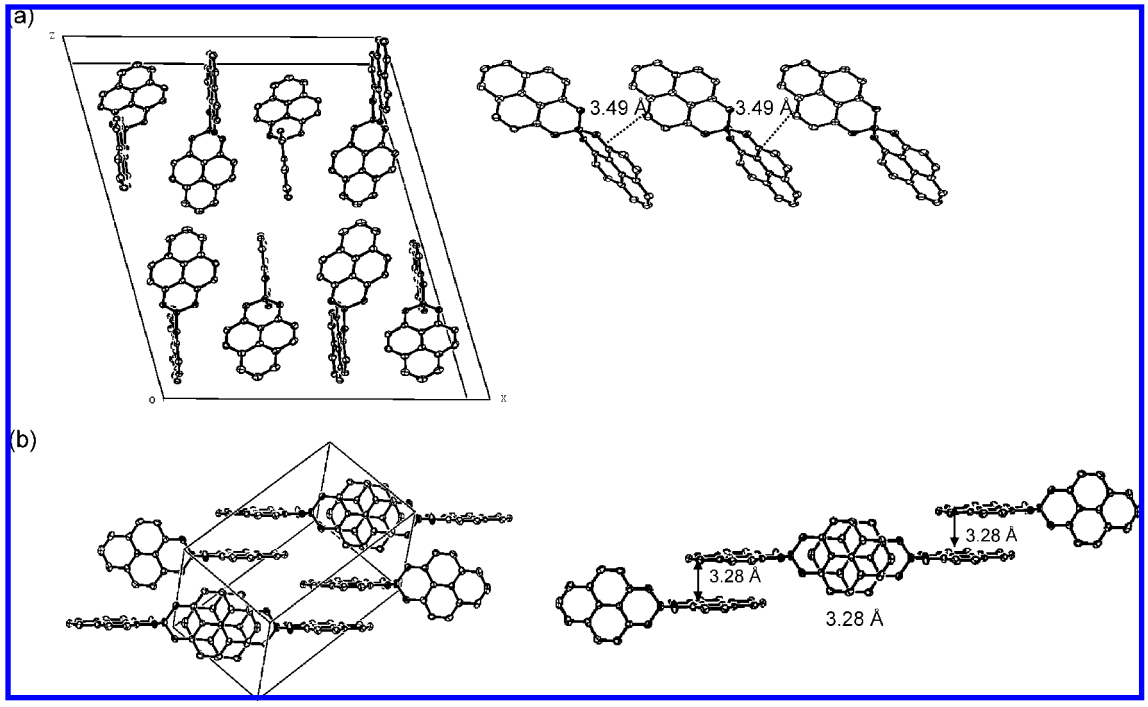

Figure 6. (a) Solid state structure of monomeric n-hexyl radical (**4**), showing the unit cell and the packing motif with the closest distance (3.49 Å) between spin bearing carbon atoms. (b) Solid state structure of π-chain cyclohexyl radical (**7**), showing the unit cell and chain structure (interplanar separation of 3.28 Å). Cyclohexyl and n-hexyl groups are omitted for clarity.

electronic structure where the odd electrons are paired in a diamagnetic π-dimer involving the superimposed phenalenyl rings.[34,35,46] Reference to Table 1 shows that the electronic structure is far more complicated and only at room temperature

Table 3. Calculated Partial Bond Orders (p^f_{kl}) in the SOMO for **1**−**10** (N,O), **11**−**13** (N,N), and **14**, **15** (O,O) Radicals

bonds	p^f_{kl} (N,O)	p^f_{kl} (N,N)	p^f_{kl} (O,O)
C1−C2	0.0519	0.0588	0.0514
C2−C3	−0.0580	−0.0669	−0.0553
C3−C3A	0.0272	0.0344	0.0281
C3A−C4	−0.0279	−0.0365	−0.0292
C4−C5	−0.0053	0	0
C5−C6	0.0053	0	0
C6−C6A	−0.0380	−0.0365	−0.0292
C6A−C7	0.0362	0.0344	0.0281
C7−C8	−0.0660	−0.0669	−0.0553
C8−C9	0.0592	0.0588	0.0514
C9−C9A	0.0086	0	0
C9A−C1	−0.0088	0	0
C9A−C9B	0.0001	0	0
C9B−C3A	0.0002	0	0
C9B−C6A	−0.0003	0	0
C1−O or C1−N	−0.0683	−0.0840	−0.0749
C9−N or C9−O	−0.0918	−0.0840	−0.0749

is the situation depicted in **14a** and **14b** of Scheme 2 actually realized (in which the odd electron is uniquely associated with a single phenalenyl FMO). According to our analysis, the unpaired spin is partially delocalized over the two phenalenyl FMOs in the individual molecules at all temperatures below about 200 K.

In Figure 4 we show the relationship between the electron density in the superimposed PLY units and their interplanar spacing; the results indicate the presence of significant electron density in the nonsuperimposed phenalenyl units even at the very lowest temperature (20 K). In fact the data suggest that the π-dimer is quite strongly bound up to ∼135 K and at 130 K the odd electron is evenly delocalized over both PLY units in each molecule; at this temperature the π-dimer is bound by 1/2 of an electron from each of the superimposed PLY units for a total count of 1 electron in the π-dimer bond.

This type of situation has been encountered previously in experimental solution studies and theoretical calculations on the π-binding between pairs of PLY radicals (π-PLY_2) and between a PLY radical and a PLY cation (π-PLY_2^+);[19,51] a number of structural studies on (π-PLY_2) are also available.[11,13,52] The binding of the PLY ring systems in π-PLY_2 and π-PLY_2^+ is found to be quite strong in both the solution and gas phases, but in the case of the charged 1-electron-bound π-PLY_2^+ system, solvation effects are important in interpreting the solution result.[19] Nevertheless this analysis supports the idea that in the solid state a single electron is sufficient to bind the π-dimer as shown in Figure 4. However, it seems that the structural transition occurs quite abruptly once the electron density in the π-dimer falls below ∼0.8 and at a temperature of 140 K the total electron count in the dimeric unit has fallen to 0.34 and continues to decrease up to room temperature at which point the electron density resides solely on the nonsuperimposed phenalenyl units.

In Figure 5 we show the magnetic and conductivity data previously reported for (**1**),[34,35] together with plots of the charge density in the nonsuperimposed PLY units and the interplanar separation of superimposed PLY rings as a function of temperature. The Curie spin count obtained from the magnetic susceptibility data in the high temperature regime correlates closely with the electron density distribution obtained from the structural analysis. At lower temperatures, in the range 90−150 K, where the system is more highly delocalized the Curie spin count is below the calculated charge (and spin) density in the nonsuperimposed PLY units, although these quantities match quite well at the lowest temperature that we could access (20 K). In the intermediate region (90−150 K) two possible explanations could be advanced for this discrepancy: in fact it is in this regime that the conductivity is enhanced by about 2 orders of magnitude and thus the Curie spin count may be subject to Pauli limiting as band effects cut off the contribution of the free spins to those in the vicinity of the Fermi level—a number of the more highly conducting π-chain radical compounds show the low, temperature-independent paramagnetism which is characteristic of Pauli susceptibility (**7**, **8**, **14**, **15**).[39,44,45] This explanation relies on solid state effects, but there is prior theoretical work that suggests that the wave function of the isolated delocalized π-dimer may be quite complex and thus the electron density may be expected to depart from the Curie spin count.[19,24,25,53,54] Nevertheless the electron (and spin) density distribution inferred from the structural analysis below 150 K offers an obvious explanation for the enhanced conductivity observed in **1** in this temperature range, as it is now clear that the dimerization process does not quench the spins to give a simple diamagnetic π-dimer ground-state as was previously assumed.[34,35] The optical properties[35] and the anomaly in the specific heat[55] at the phase transition are also explained by the current model, but we defer the discussion of these quantities to a future publication.

The regression analysis for the remaining radicals (**2**−**15**) is given in Table 2; the other boron-based radicals which adopt the π-dimer structure (**2**, **3**, **5**, and **9**) are readily analyzed in terms of the paradigm established above for **1**. The solid state structures of radicals **2** (293K) and **5** (223 K) are clearly fully paramagnetic weak π-dimers in which the unpaired electrons reside solely in the nonsuperimposed PLY units. They show mean plane separations for the superimposed PLY units of D = 3.4 Å, and maintain a Curie magnetic susceptibility down to 30 K and there exists little indication of electronic interaction;[37,38] similar remarks apply to the tris-radical **10** although the Curie spin count is low for this compound.[40] The structure of **3** at 173 K indicates a strong π-dimer (D = 3.12 Å), with the unpaired electron fully localized at the superimposed PLY units and this is consistent with the experimental magnetic susceptibility data.[34,35] At 100 K radical **9** is a strong π-dimer which exhibits limited electron delocalization and the magnetic susceptibility measurements indicate that the Curie spin count is low over the whole temperature range.[39]

The monomeric radicals also offer some surprises, particularly in the case of radicals **4**, (Figure 6a) **12**, and **13**, which have no intermolecular contacts within van der Waals atomic separation; nevertheless, all three of these radicals are found to have an asymmetric electron density distribution. The only monomeric radical which is fully delocalized according to the structural

(48) Streitwieser, A. *Molecular Orbital Theory for Organic Chemists*; John Wiley: New York, 1962.
(49) Salem, L. *The Molecular Orbital Theory of Conjugated Systems*; W. A. Benjamin, Inc: New York, 1966.
(50) Yates, K. *Huckel Molecular Orbital Theory*; Academic Press, Inc.: New York, 1978.
(51) Lu, J.; Rosokha, S. V.; Kochi, J. K. *J. Am. Chem. Soc.* **2003**, *125*, 12161–12171.
(52) Beer, L.; Mandal, S. K.; Reed, R. W.; Oakley, R. T.; Tham, F. S.; Donnadieu, B.; Haddon, R. C. *Cryst. Growth Des.* **2007**, *7*, 802–809.
(53) Borden, W. T.; Iwamura, H.; Berson, J. A. *Acc. Chem. Res.* **1994**, *27*, 109–116.
(54) Jung, Y.; Head-Gordon, M. *J. Phys. Chem. A* **2003**, *107*, 7475–7481.
(55) Jorge, G. A.; Kim, K. H.; Jaime, M.; Chi, X.; Hellman, F.; Itkis, M. E.; Mandal, S. K.; Haddon, R. C. *AIP Conf. Proc.* **2006**, *850*, 1315–1316.

analysis is radical **11**, which has intermolecular contacts just below the van der Waals separation for carbon atoms (3.38 Å); all four of the radicals (**4**, **11**, **12**, and **13**) are paramagnetic with near-Curie−Weiss spin susceptibilities.[32,33]

The radicals with infinite $\pi-\pi$ interactions (**6**−**8**, **14**, and **15**) (Figure 6b) are fully delocalized (as required by symmetry in most cases), but even **15** which possesses both superimposed and partially superimposed π-dimer overlaps in the π-chain shows a highly delocalized electron density distribution and we have interpreted the electronic structure of these radicals in terms of a resonating valence bond ground state.[39,44,45] The π-chain radicals (**7**, **8**, **14**, and **15**) are the most highly conducting radicals that we have isolated to date and their magnetic susceptibilities are in accord with Pauli paramagnetism and may also be fit with the 1-D Heisenberg antiferromagnetic chain model. The benzyl radical (**6**) has a unique π-step structure in which only 1/3 of the active carbon atoms are involved in π-π interactions and it may be seen that this reduces the symmetry of the PLY unit to the point that the compound is not well described by the structural model as evidenced by the low correlation coefficient (Table 2).

Conclusions

By exploiting the relationship between bond order and bond length we are able to identify the degree of spin and charge density (de)localization in the phenalenyl-based radical conductors and this has allowed us to understand some of the unexplained features of the electronic structure and physical properties while bringing to light other unanticipated subtleties. In particular we were able to show that the enhanced conductivity in the ethyl (**1**) and butyl (**3**) radicals at the magnetic phase transition is the result of a complex, but delocalized electronic structure and not the formation of a diamagnetic π-dimer. The analysis also suggests a revision in our view of the electronic structure of some of the monomeric radicals, in spite of the fact that **4**, **12**, and **13** have no intermolecular contacts within van der Waals atomic separation, all three of these radicals are found to have an asymmetric electron density distribution. Radical **11** proved to be the only monomeric radical which is fully delocalized. As expected, the π-chain radicals (**7**, **8**, **14**, and **15**) are delocalized resonating valence bond structures and these are the most highly conducting radicals that we have isolated. Thus the phenalenyl-based radical conductors (**1**−**15**) span a broad range of electronic structures with respect to the molecular-level (de)localization of the spin and charge density and have already produced a fascinating array of physical properties.

Experimental and Calculation Section

Preparation of Radical 1. Bis(9-*N*-ethylamino-1-oxo-phenalene) boron, **1**, was prepared and crystallized according to literature procedure.[34]

X-ray Crystallography. A black needle fragment (0.47 × 0.19 × 0.13 mm^3) of **1** was used for the single crystal X-ray diffraction study. The crystal was mounted on to a glass fiber with epoxy resin. X-ray intensity data were collected at 90 (2), 100 (2), 110 (2), 120 (2), 130 (2), 135 (2), 140 (2), 150 (2), 160 (2), 170 (2), and 293 (2) K, on a Bruker APEX2 (version 2.0−22) platform-CCD X-ray diffractometer system (Mo-radiation, $\lambda = 0.71073$ Å, 50 KV/40 mA power).[56] Absorption corrections were applied to the raw intensity data using the SADABS program.[57] The Bruker SHELXTL (Version 6.14) software package was used for phase determination and structure refinement.[58] Atomic coordinates, isotropic, and anisotropic displacement parameters of all the non-hydrogen atoms were refined by means of a full matrix least-squares procedure on F^2. All H-atoms were included in the refinement in calculated positions riding on the atoms to which they were attached.

We have included in the Supporting Information a plot of the diagonal anisotropic displacement parameters (ADP) of one of the PLY ring carbon atoms of **1** that is involved in the dimerization process as function of temperature together with a comparison plot of data taken from the literature of the same quantities in a semibullvalene derivative where there is known to be equilibrating isomers present in the lattice (Figures S17−S19). If the fully delocalized structure of **1** at ∼130 K were in fact an average of two disordered structures, one might expect it to have unusually large ADP values compared to the more localized structures at the flanking temperatures. In fact, the diagonal ADP tensor elements show approximately linear thermal increase over this range, which argues against the disorder interpretation and in favor of our interpretation in terms of full static delocalization. Thus the analysis shows quite conclusively the presence of a fully delocalized static structure in the vicinity of the magnetic phase transition and we are indebted to a referee for this observation.

Calculations. The calculated partial bond orders (p^f_{kl}) are given in Table 3, based on standard HMO parameters.[48,59] The bond length differences (Δr_{kl}) between radical and cations are included in the Supporting Information; The structures of the radicals, (reference cations) were taken from: **1**,[34] (**3**$^{+46}$); **2**,[37] (**3**$^{+}$); **3**,[34] (**3**+); **4**,[32] (**3**+); **5**,[38] (**5**$^{+38}$); **6**,[41] (**6**$^{+41}$); **7**,[44] (**7**$^{+44}$); **8**,[39] (**8**$^{+39}$); **9**,[39] (**7**+); **10**,[40] (**10**$^{+40}$); **11**,[33] (**11**$^{+33}$); **12**,[33] (**11**+); **13**,[33] (**11**+); **14**,[45] (**14**$^{+45}$); **15**,[45] (**15**$^{+45}$).

Acknowledgment. This work was supported by the Office of Basic Energy Sciences, Department of Energy, under Grant DE-FG02-04ER46138.

Supporting Information Available: Plots of the differential change in bond order (p^f_{kl}, x) versus bond length (Δr_{kl}, y) in the form $y = a_\beta x$ with bond length and Δr_{kl} values for radicals **1**−**15**; π-bond order versus bond length plot and corresponding table for ovalene molecule; anisotropic displacement parameters (ADP) vs temperature plots of C(1) atom of radical **1** and C(4) atom of semibullvalene; full literature citation for ref 4; crystallographic CIF files for 90−293 K data of radical **1**. This material is available free of charge via the Internet at http://pubs.acs.org.

JA8037307

(56) *APEx2 Software Reference Manual, 2.0−22*; Bruker Analytical X-ray System, Inc: Madison, WI, 2004.
(57) *SADABS Software Reference Manual 2004/1*; Bruker Analytical X-Ray System, Inc: Madison, WI, 2004.
(58) *SHELXTL Software Reference Manual, 6.14*; Bruker Analytical X-Ray System, Inc: Madison, WI, 2008.
(59) Haddon, R. C. *J. Am. Chem. Soc.* **1980**, *102*, 1807–1811.